Application of Voronoi Tessellation of Spherical Surface to Geometrical Models of Skeleton Forms of Spherical Radiolaria

Takashi Yoshino[1]*, Atsushi Matsuoka[2], Toshiyuki Kurihara[3], Naoto Ishida[4], Naoko Kishimoto[5], Katsunori Kimoto[6] and Shu Matsuura[7]

[1]*Department of Mechanical Engineering, Toyo University, Japan*
[2]*Department of Geology, Faculty of Science, Niigata University, Japan*
[3]*Graduate School of Science and Technology, Niigata University, Japan*
[4]*Venture Business Laboratory, Niigata University, Japan*
[5]*Department of Mechanical Engineering, Setsunan University, Japan*
[6]*Research Institute for Global Change (RIGC), Japan Agency for Marine-Earth Science and Technology (JAMSTEC), Japan*
[7]*Faculty of Education, Tokyo Gakugei University, Japan*
*E-mail address: tyoshino@toyo.jp

We investigated two geometrical models of skeleton forms of spherical radiolaria. Both models are based on Voronoi tessellation of given points on a sphere. We allocate a given number of points called "generators", which can be related to pore frames, and obtained their Voronoi tessellation and approximated polyhedron. The first model is based on random allocation of generators, and the second one is based on global minimization of a potential function whose value is calculated from a generator distribution. Depending on the types of these generator distributions, we obtained different types of approximated polyhedrons. Using these polyhedrons, we analyzed the frequency distributions of the number of vertices of the polygons and the total edge lengths. We then compared the polyhedrons derived by the tessellation with real radiolaria. A comparison of frequency distributions revealed that the first model is not sufficient for mesh-like radiolaria. However, the second model had similar distribution to that of another type of spherical radiolaria which has almost regular structure. Under the condition of same number of generators, the second model produces approximately 6 percent smaller total edge length than the first model.
Key words: Spherical Radiolaria, Voronoi Tessellation, Geometrical Model, Skeleton Form

1. Introduction

Skeleton form is an important factor when analyzing the evolution of an organism for the following two reasons. Because the skeleton shape is recorded in sedimentary rocks, its evolutionary history can be directly observed. Also, because the skeleton is the hardest material which organisms form, it is thought to relate to some mechanical functions of the living organism. In order to understand the role of the skeleton in detail, its geometrical properties must be known.

The present study focuses on a skeleton-forming model of spherical radiolaria. Radiolaria exhibit a variety of shapes (De Wever *et al.*, 2001). Their skeletons are used for determining geological time and environment of past oceans. Despite their geological importance, their ecology remains unclear (Matsuoka, 2007).

We considered spherical radiolaria especially single-layered spherical spumellaria because of the simplicity of their form. As described above, the skeleton form of radiolaria varies greatly, and so it is hard to discuss a general strategy of skeletogenesis. Fortunately, in some cases of radiolaria, the skeleton is composed of silica; thus, we ignore reconstruction of the skeleton after it was first formed: the formation of the initial skeleton is believed to be related to

the construction plan of the final form.

On the other hand, pattern formation on a sphere has been widely studied. The surface of the Earth is a representative example of such pattern formations (Turcotte and Schubert, 2001). Erber and Hockney (1991) reported statistical distributions of charged particles on a spherical surface. They obtained these distributions by using the steepest descent method to minimize the electrostatic (Coulomb) potential function. Tanemura (1998, 2008) proposed an algorithm for skeleton formation of spherical radiolaria. His model is based on a theorem of spherical geometry called Lexell's circle. Using this theorem, the algorithm sequentially allocates vertices to compose almost regular polyhedrons. Because the method consists of repeated improvement of the local configuration, the obtained configurations are considered to be local minimum solutions.

In the present study, we applied the concept of the Voronoi tessellation to skeleton form. We introduced two types of spherical point distributions for obtaining skeleton-like polyhedrons and discuss some of the properties of the obtained ones. Figures 1(a) and (b) show real examples of radiolaria considered in this study. We recognize them as extreme cases of radiolarian skeleton structures. *Cyrtidosphaera reticulata* Haeckel (Fig. 1(a)) is an example of random structure and *Acanthosphaera circopora* Popofsky
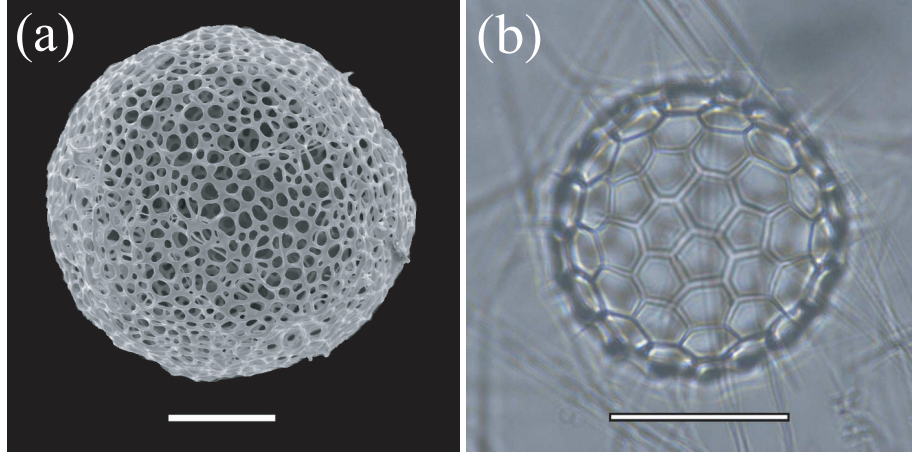
Fig. 1. Photographs of spherical radiolaria considered in this study. (a) *Cyrtidosphaera reticulata* Haeckel. (b) *Acanthosphaera circopora* Popofsky. Scale bars indicate 50 μm.
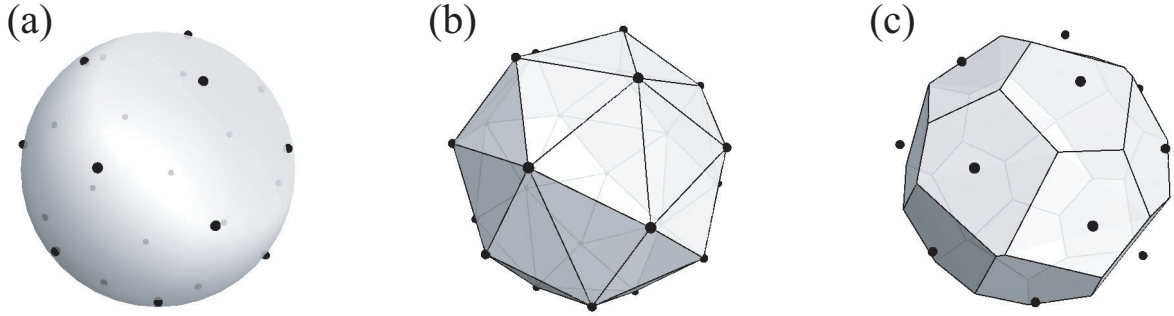

Fig. 2. Correspondence of spherical points. (a)Example of the generators on the sphere ($N = 24$). (b) Convex hull of the generators (a). (c) The dual polyhedron of the polyhedron (b).

(Fig. 1(b)) is that of regular one. Both species are frequently observed in the sea off Sado Island of Japan. Because many spherical radiolaria are characterized by intermediate structure between random and regular structures, the two extreme examples must be described by the same concepts of geometrical model in order to describe whole skeleton structures of spherical radiolaria.

2.   Mathematical Model of Spherical Radiolaria
2.1   Basic Concepts

We approximate the skeleton of spherical radiolaria with edges of convex polyhedron, ignoring section width because our focus is geometrical features rather than mechanical ones. Throughout this study, we assumed that the vertices of the polyhedron are allocated on the surface of the unit sphere. In the following, we use the set of given points on the sphere $\mathbf{r}$,

$$\mathbf{r} = (\mathbf{r}_1, \mathbf{r}_2, \cdots, \mathbf{r}_N), \qquad (1)$$

where $\mathbf{r}_i$ is a location of the i-th point on the unit sphere and N is number of the the points. Each $\mathbf{r}_i$ has three components (x_i, y_i, z_i) in Cartesian coordinates and they satisfy the relation,

$$x_i^2 + y_i^2 + z_i^2 = 1.$$

We call each point and the set of the points "generator" and "generators", respectively. The distribution of generators determines the geometry of convex polyhedron as described in the following.

One of the basic ideas of polyhedron construction herein is to make a convex hull of generators randomly allocated on a sphere. A convex hull of given set $\mathbf{r}$ is the set of points $\mathbf{x}$ which satisfies the relation,

$$\mathbf{x} = \lambda_1\mathbf{r}_1 + \lambda_2\mathbf{r}_2 + \lambda_3\mathbf{r}_3 + \cdots + \lambda_N\mathbf{r}_N, \qquad (2)$$

where $\lambda_i \geq 0$ for all i and $\sum_{i=1}^{N} \lambda_i = 1$ (Okabe *et al.*, 2000). In Fig. 2(b), we give an example of the convex hull of the generators shown in Fig. 2(a). A convex hull of the generators $\mathbf{r}$ is the smallest convex polyhedron which contain all generators either in or on it. In a case that all generators are allocated randomly on sphere, all generators correspond to vertices of their convex hull. The adjacent vertices of each vertex (generator) are sometimes called Voronoi neighbors. As mentioned in following results, the
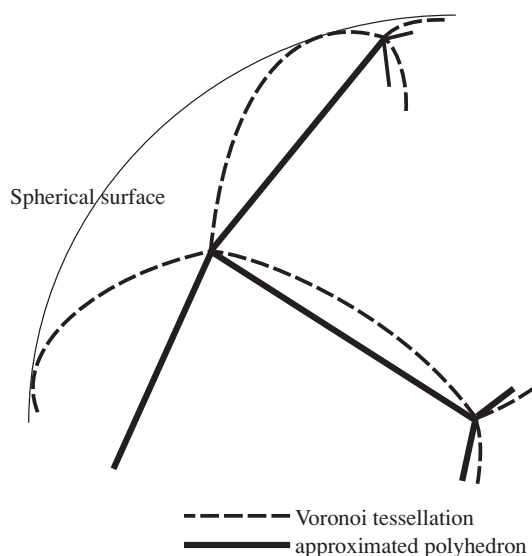
Fig. 3. Concept of approximated polyhedrons. Dashed lines denote the tessellation and solid lines denote the approximated polyhedron. The approximated polyhedron is obtained by replacing the arcs of Voronoi tessellation with lines.

convex hull is not a good model for spherical radiolarian skeletons because the obtained polyhedrons are different from the skeleton forms of radiolarian as shown in Fig. 1.

Another way to construct polyhedrons similar to skeleton forms of spherical radiolarian is to form a dual polyhedron of a given convex hull. The dual polyhedron, or the polar polyhedron, has one-to-one correspondences with the original one: these are 1) each vertex of the dual polyhedron corresponds to a face of the original polyhedron, 2) each edge of the dual corresponds to an edge of the original one, and 3) each face of the dual corresponds to a vertex of the original one. The formal definition of a dual polyhedron is given in textbooks on polyhedron geometry (e.g., that of Coxeter, 1989). The relationships of generators, their convex hull, and the dual polyhedron are illustrated in Fig. 2. As shown in Fig. 2, the dual polyhedron is determined when convex hull of the generators are determined.

In order to construct dual polyhedron, we use the idea of Voronoi tessellation. It is known that the Voronoi tessellation is one of the method for constructing dual polyhedron (Renka, 1984; Okabe *et al.*, 2000). As shown in Fig. 3, although the boundaries of the Voronoi tessellation on spherical surface are arcs of great circles, we replaced these arcs with lines because we are approximating skeleton forms with polyhedrons. We refer to the resultant polyhedron as an "approximated Voronoi polyhedron" or "approximated polyhedron". This approximation was carried out throughout this study. Figure 3 illustrates part of a sphere, a Voronoi tessellation, and its approximated Voronoi polyhedron. We uses the term "approximated Voronoi polyhedron" because the term "Voronoi polyhedron" corresponds to a cell of three dimensional Voronoi tessellation.

Neglecting the difference of edge type, construction of convex hull using the generators is equivalent to construction of Delaunay triangulation (Okabe *et al.*, 2000). Therefore, it is possible to obtain the Delaunay triangulation of

the set by using the algorithm of three dimensional convex hull which we used in this study. Furthermore, Voronoi tessellation of the generators is obtained from the result of Delaunay triangulation (Okabe *et al.*, 2000). Therefore, the procedure to obtain the approximated Voronoi polyhedron of given generators are summarized as follows. Firstly, we obtain the convex hull of the generators. Secondary, we acquire all equations of planes perpendicular to and containing the location vector. Therefore, each plane is corresponded to each generator. Finally, we obtain the intersection lines of adjacent pairs, Voronoi neighbors in other words, of the convex hull's vertices. The lines correspond to the edges of the approximated Voronoi polyhedron of given generators. also allocated on the unit sphere. The polyhedron obtained by this procedure is the dual polyhedron of convex hull because the obtained polyhedron satisfies the features of dual polyhedron described above.

In order to compare the simulation results with 2D skeleton images quantitatively, we estimated the frequency distribution of polygons from the 2D images. Because the value of N directly affects the result, estimation of an appropriate number is important. The procedure of the estimation is summarized as follows: First, we approximated the outline of the skeleton image by a circle to estimate its radius and center (Fig. 4a). Second, we drew a smaller circle having the same center as the first circle (Fig. 4b). The ratio of the second radius to the first was defined as ξ. Third, we approximated the skeleton structure within the smaller circle using lines (Fig. 4c). The obtained figure can be considered to be an approximation of part of the structure of the radiolarian skeleton (Fig. 4d). Next, we counted the frequency distribution of polygons within the second circle. Because the frequencies were obtained using only part of the entire skeleton, we had to multiply them by a factor. The factor is based on the ratio of the surface area of the unit sphere to surface area of the spherical cap whose radius is ξ. In the case of Fig. 4(b) (*Cyrtidosphaera reticulata* Haeckel), $\xi = 0.764$ and the factor is approximately 5.64.

2.2 Models

Our first model is for mesh-like skeletons. We again allocated a given number of points randomly on the surface of the unit sphere and applied Voronoi tessellation in order to obtain its dual polyhedron. The generators correspond to the pore frames of radiolaria uniformly distributed on the sphere. Hereafter, we call an approximated Voronoi polyhedron obtained from a random generator distribution a "random approximated Voronoi polyhedron" (RAVP).

In order to consider another type of radiolarian skeleton, almost regular polyhedrons, we introduce a new model and examine its applicability. Some radiolaria have skeletons similar to regular polyhedrons. In our polyhedron model, such regular structures are expected to appear from the generators distributed more homogeneously. Here, we introduce generators that interact with each other and seek a potential minimum configuration of points on the surface of the sphere. In other words, we assumed that the generators on the sphere interact through some type of potential energy. The distributions of generators are determined by the potential function, which is the sum of the potential energies over all pairs of generators.
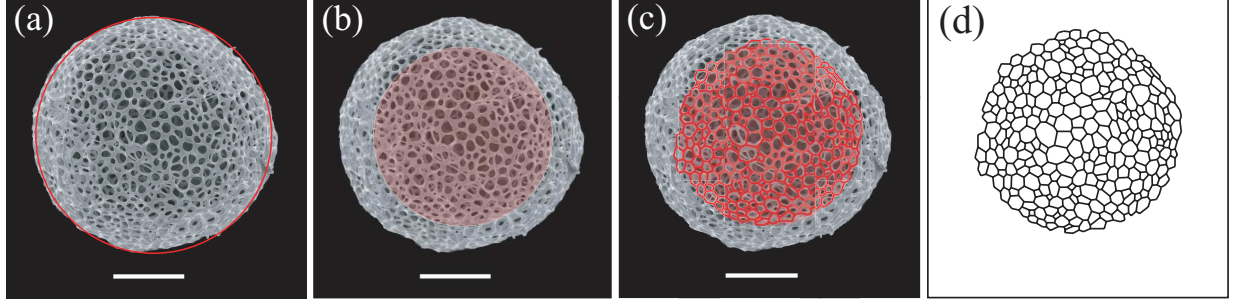
Fig. 4. Procedure for estimating the frequency distribution of polygons of the image of the real radiolarian. The estimated frequency distribution is the that of (d) times surface ratio of the approximated sphere (a) to the spherical cap (b). Scale bar indicates 50 μm.
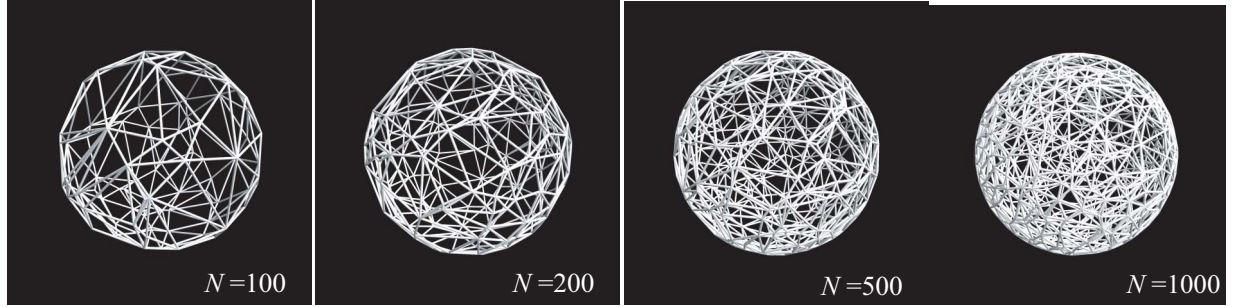

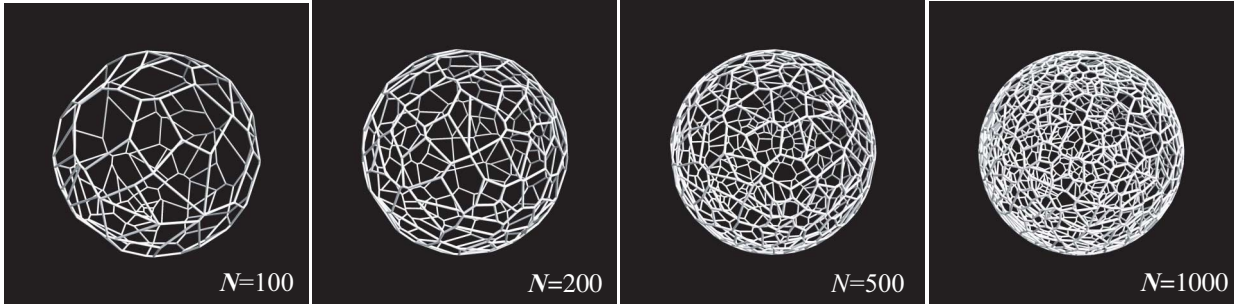Fig. 5. Examples of convex hulls of random generators on a spherical surface ($N = 100, 200, 500,$ and 1000).

Fig. 6. Examples of RAVP ($N = 100, 200, 500,$ and 1000). The polyhedrons were generated from the same generators in Fig. 5 and so that they are dual polyhedrons of those polyhedrons.

Because we consider a spherical skeleton, which does not have a characteristic direction, all generators can be considered to be equivalent. In other words, there is no characteristic point among them. This assumption corresponds to the condition in which each point has the same electronic charge for the case of a Coulomb potential. We call the new model "minimum potential approximated Voronoi polyhedrons" (MPAVP). The concept of generator distribution of this model is identical to the Erber and Hockney model (Erber and Hockney, 1991) if we choose the Coulomb potential as the potential function and use the steepest descend method to obtain the generator distribution.

We used sums of power functions as the potential functions. The potential functions are defined by

$$U_n(\mathbf{r}) = \sum_{<i,j>} \frac{1}{\left|\mathbf{r}_i - \mathbf{r}_j\right|^n}, \qquad (3)$$

where the summation is over all pairs. We consider the three cases $n = 1, 6,$ and 12 in this study. The case $n = 1$ corresponds to the electrostatic potential (long-range interaction) and the other cases are frequently used to represent of short-range interactions.

We obtained optimized configurations of spherical points by using the simulated annealing method [**?**], which derives an almost globally optimized generator distribution for a given potential function. The procedure is summarized as follows: (A) A given number of random points are generated on a unit sphere. (B) A parameter β (inverse temperature) is set to an initial value. (C) A candidate point is selected sequentially from among the current points and is released to walk at random. (D) The difference between the potential values of ΔU_n for the candidate and the current configuration is calculated. (E) A random number ξ in the
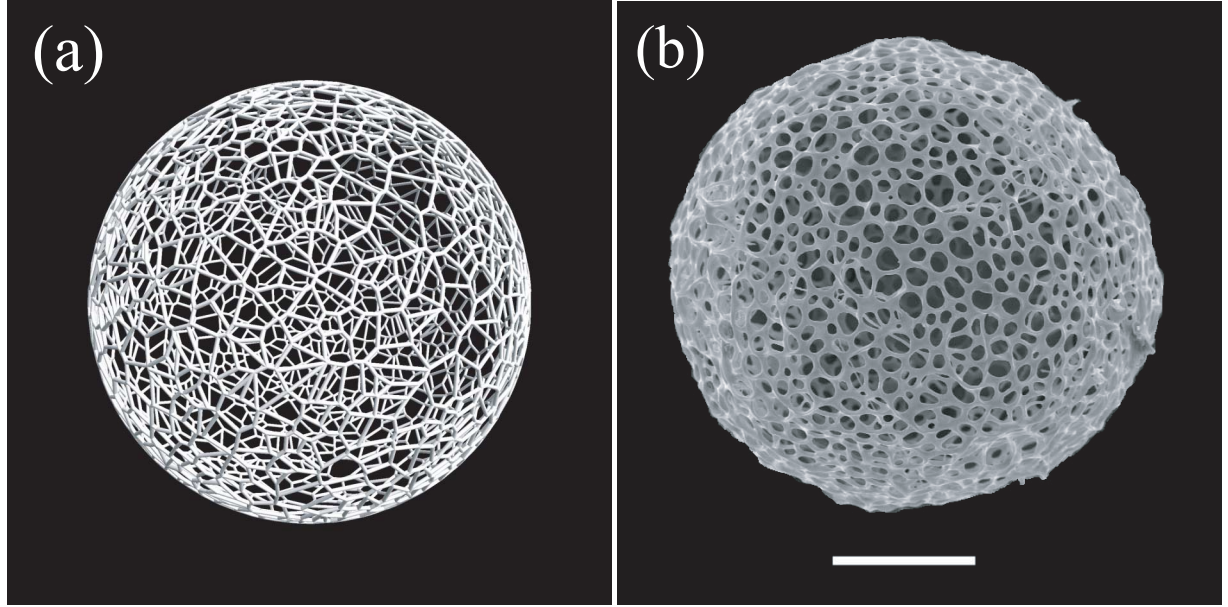
Fig. 7. Comparison of the simulation result of RAVP for $N = 1540$ with a real mesh-like radioralia (*Cyrtidosphaera reticulata* Haeckel). Scale bar indicates 50 μm.
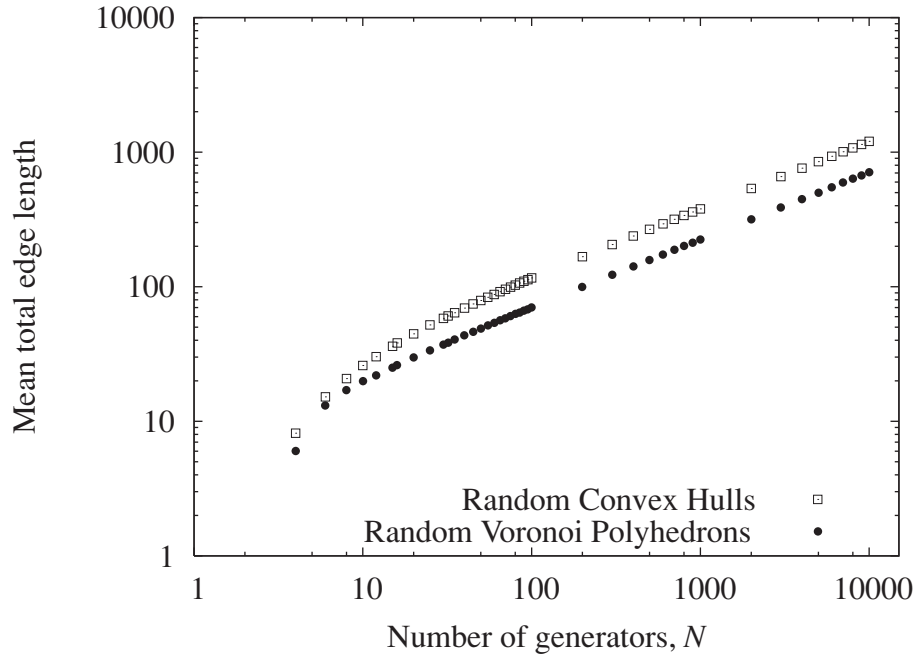

Fig. 8. Comparison of N dependence of mean total edge length of convex hulls and Voronoi tessellations (RAVP) with same random generator distributions.

range $[0, 1)$ is generated, and a new point is chosen according to the rule: if $\xi \leq \exp(\beta \Delta U_n)$, the candidate point is accepted; otherwise, it is rejected. (F) If the system is not yet stable, return to (C). (G) The parameter β is increased by $\Delta\beta$. (H) (C) through (F) are continued until β reaches the terminal value.

Rapid annealing causes local minimization. In order to avoid this, we increase the value of β linearly and set the increment of increase sufficiently small. Furthermore, we prepare a sufficient number of Monte Carlo steps for each β. We chose the initial value of β as 0, the terminal value as 500, and the increment $\Delta\beta$ as 10. The number of Monte Carlo steps was set at 20000; therefore, $20000 \times N$ candidates were tested for each β. The variance of the potential function was large for small β and decreased to small values when β became large. A cube was formed for $N = 6$, and a dodecahedron for $N = 12$. These proved the suitability of our annealing schedule.
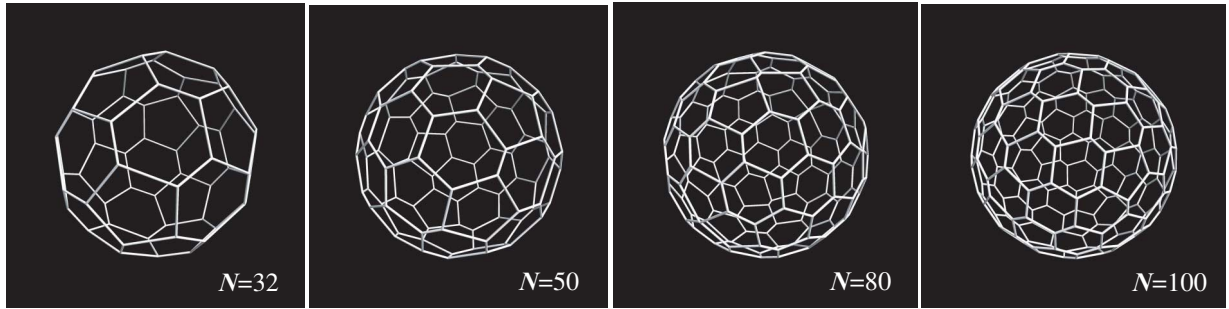
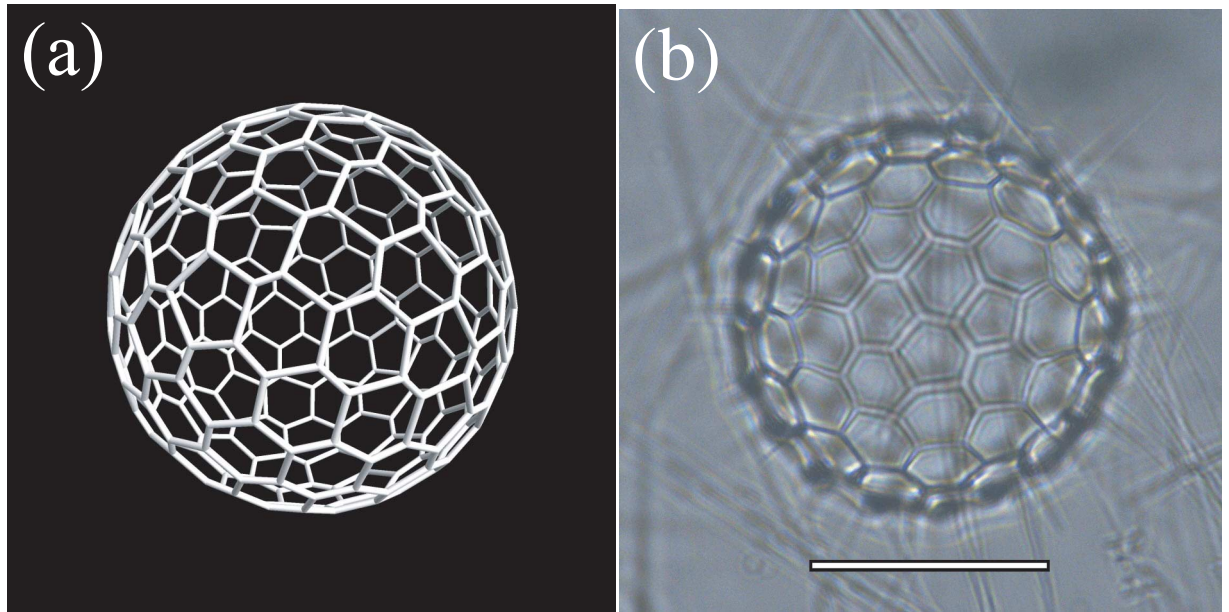Fig. 9. Examples of polyhedrons obtained from the MPAVP ($n = 1$) model ($N = 32$, 50, 80, and 100).

Fig. 10. Comparison of an example of a MPVAP ($N = 138$ and $n = 1$) with almost-regular type of spherical radiolarian (*Acanthosphaera circopora* Popofsky). Scale bar indicates 50 μm.

3. Results

Figure 5 shows some examples of convex hull of generators randomly allocated on the sphere for different numbers of points N. The obtained polyhedrons have two features: most vertices have mainly 6 associated edges, and almost all the faces are triangles. These results are consistent with Euler's theorem of convex polyhedrons. From the viewpoint of cost minimization of skeleton-forming materials, the resultant skeletons are clearly not optimal. Furthermore, such polyhedrons are not similar to any types of real spherical radiolaria. From this, we conclude that this model is not appropriate for spherical radiolaria.

Figure 6 shows examples of numerical results for the approximated Voronoi polyhedrons generated by randomly allocated generators on sphere (RAVP). The generator distributions of the examples were same ones with the point distributions of examples in Fig. 5. Because of the duality, the polyhedrons consist mainly of hexagons with vertices of degree three. one.

Comparison of a numerical result for $N = 1540$ and a real sample (*Cyrtidosphaera reticulata* Haeckel) is shown

in Fig. 7. The value 1540 was estimated from the 2D image in Fig. 1(a) as mentioned above. The result was similar to a type of radiolarian that has a mesh-like skeleton intuitively.

In order to consider the features of the random approximated Voronoi polygons (RAVPs), we compared the mean total edge lengths of the polyhedrons with those of convex hulls for each N. We generated 100 samples of spherical random points and calculated their convex hulls and RAVPs. Then, we obtained mean total edge lengths for both the convex hulls and RAVPs. The results are shown in Fig. 8. The mean total edge length of the RAVP is smaller than that of the convex hull for all N's except for $N = 4$ and 5. For small values of N, oblate polyhedrons are produced frequently so that the mean value of the total edge length of RAVP can also be smaller than those of random convex hulls.

Examples of the resulting polyhedrons of MPAVP, our another model, are shown in Fig. 9. The obtained polyhedrons consist only of nearly regular pentagons and hexagons. We also observed a striking similarity between the $N = 138$ polyhedrons and a real spherical radiolaria
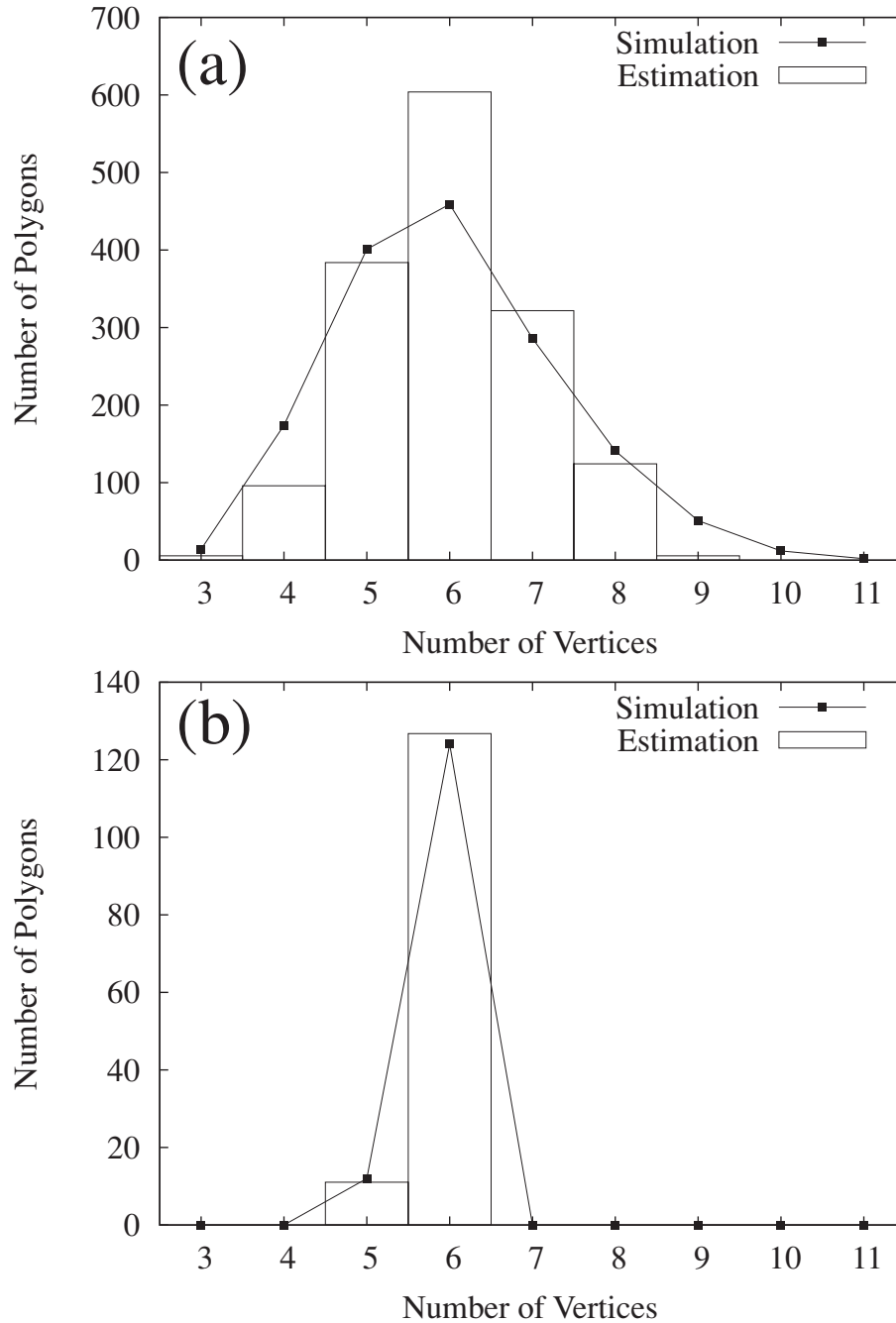
Fig. 11. Comparison of number of vertices frequency distributions of simulation result with that of radiolarians estimated from 2D images. a) RAVP(Fig. 7, $N = 1340$) , b) MPAVP (Fig. 10, N=138 and $n = 1$).

(*Acanthosphaera circopora* Popofsky) in Fig. 10. The value 138 was chosen by estimation from the 2D image described above.

The observed skeleton also consists only of pentagons and hexagons in the case of *Acanthosphaera circopora* Popofsky (Fig. 10). According the Euler's formula, the exact number of pentagons should be 12 under the assumption that all vertices are degree three. In the shown example, the estimated number of faces is 138 and the number of pentagons is 11. Nevertheless, although the estimated number of pentagons is not consistent with analytical estimation, its value is very similar. For this reason, we conclude that the

estimation procedure works well. All of the pentagons are isolated in the cases of both the observed skeleton structure and the simulation result for MPAVP. It is notable that here we examined only frequency distribution not configuration (arrangement of polygons).

The estimated frequency distribution of polygons was compared with the simulation result of RAVP for the case of (*Cyrtidosphaera reticulata* Haeckel) (Fig. 10) in Fig. 11(a). We also showed comparison in cases of MPAVP in Fig. 11(b) mentioned above. In order to avoid the dependence on the number of generators, we set the number of generators to 1574, which is the number of faces estimated from
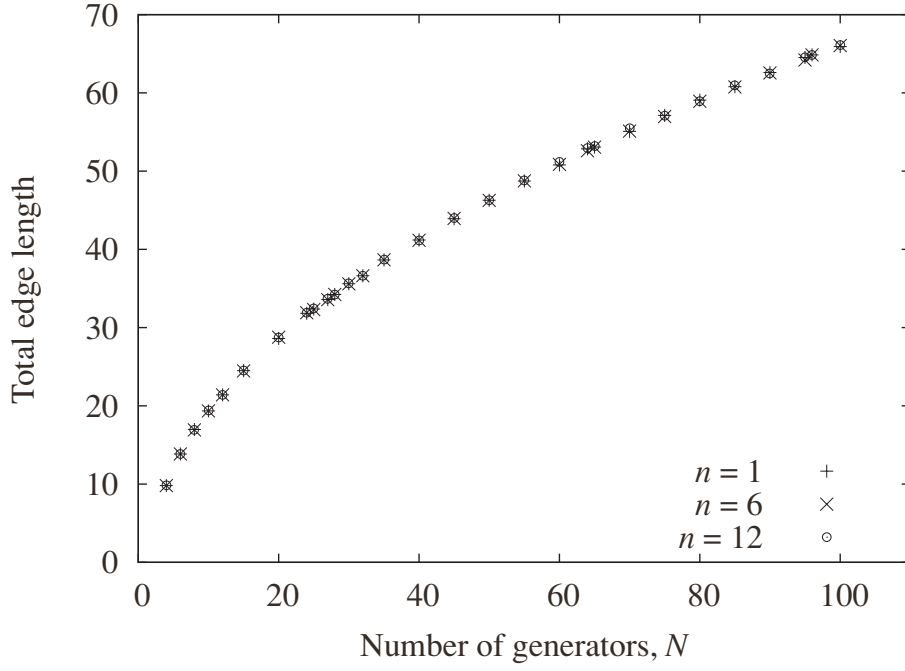
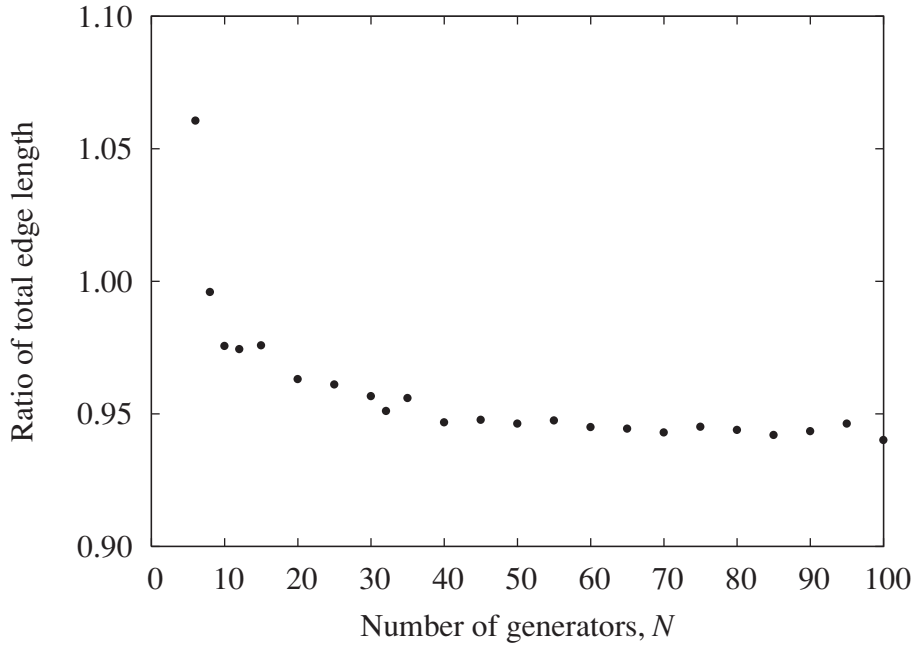Fig. 12. Total edge length of the minimum potential model for different exponents ($n = 1$, 6, and 12).

Fig. 13. N dependence of total edge length ratio of MPAVP ($n = 1$) to RAVP.

Fig. 1(a) using our method described in Section 2. Figure 11(a) shows that the two frequency distributions are different. In cases that the number of vertices are 6 and 7, the frequencies of RAVP are smaller than those of the estimated polyhedron. On the other hand, for both smaller and larger numbers of vertices, the frequencies of RAVP are larger. In other words, the deviation from number of vertices 6 of the numerical result is larger than that of real radiolarian. This result indicates that the RAVP model is not suitable fully

describing the properties of Fig. 1(a).

Holding the number of generators fixed, we compared the total edge lengths of the RAVP and MPAVP models. Figure 12 shows the N dependence of total edge length. The three models, $n = 1$, 6, and 12, produced almost identical values. For large N, the length grows almost linearly with N. This tendency is also observed for random Voronoi polyhedrons. We also obtained ratios of the total edge lengths of the RAVP and MPAVP. Figure 13 shows

the N dependence of this ratio. For large N, the length of MPAVP is approximately 6 percent smaller than that of RAVP. Therefore, from the viewpoint of geometry, MPAVP is effective for decreasing total edge length.

4. Discussions

We examined the two extreme models of skeleton shapes of spherical radiolaria and one model (MPAVP) is good agreement with almost regular structure. The MPAVP model can describe some types of radiolarian skeletons like *Acanthosphaera circopora* Popofsky; however, the RAVP model is not adequate for describing mesh-like radiolarian, even though Voronoi polyhedrons are similar in form to real spherical radiolaria from a qualitative point of view. According to the results, weak interaction, that is, not as strong as in the MPAVP model, may work for the force between generators for the case of mesh-like radiolaria. The appropriate form for the potential energy function of such a structure remains unclear. One idea of the improvements may be restriction of ranges of interaction such as restriction of summation of $< i, j >$ in Eq. (4).

One deficiency of our analysis is the existence of an inner shell: most spherical radiolaria consist of multiple layers of shells connected by radial beams. Because our simulation assumes no such beams, our simulation is inconsistent with the actual construction on the outer shell. The most optimistic idea is that the outer shell completely reflects the structure of inner shell, however, there is no evidence to support such an idea.

We cannot observe a qualitative difference between our results and those of Tanemura ($16 \leq N \leq 40$). In other words, a qualitative difference between local minimization and global one has not been found. Therefore, the problem relating to strategy selection for skeletogenesis of spherical radiolaria remains.

From a biological viewpoint, it is unknown whether the 6 percent difference in total edge length is large or not. In order to discuss this in detail, the mechanical properties of the skeleton form must be understood in detail.

References

Coxeter, H. S. M. (1989) *Introduction to Geometry*, Wiley.

De Wever, P., Dumitrica, P., Caulet, J. P., Nigrini, C. and Caridroit, M. (2001) *Radiolarians in the Sedimentary Record*, G & B Science Pub.

Erber, T. and Hockney, G. M. (1991) Equilibrium configurations of N equal charges on a sphere, *J. Phys. Math. Gen.*, **24**, L1369–L1377.

Kirkpatrick, S., Gelatt, C. D., Jr. and Vecchi, M. P. (1983) Optimization by simulated annealing, *Science*, **220**, 671–680.

Matsuoka, A. (2007) Living radiolarian feeding mechanisms: new light on past marine ecosystem, *Swiss J. Geosci.*, **100**, 2739–279 .

Okabe, A., Boots, B., Sugihara, K. and Chiu, S. N. (2000) *Spatial Tessellations: Concepts and Applications of Voronoi Diagrams*, 2nd ed., Wiley.

Renka, R. J. (1984a) Interpolation of data on the surface of a sphere, *ACM Transactionson Mathematical Software*, **10**, 417–435.

Renka, R. J. (1984b) Algorithm 623: interpolation on the surface of a sphere, *ACM Transactions on Mathematical Software*, **10**(4), 437–439 .

Tanemura, M. (1998) Random packing and tessellation network on the sphere, *Forma*, **13**, 99–121.

Tanemura, M. (2008) Optimal configurations on the sphere for small number of points, *Bulletin of the Society for Science on Form*, **23**, 186–187 (symposium abstract).

Turcotte, D. L. and Schubert, G. (2001) *Geodynamics*, 2nd ed., Cambridge University Press.